Available online at www.sciencedirect.com

ScienceDirect

Procedia Computer Science 4 (2011) 2226–2235

Procedia Computer Science

International Conference on Computational Science, ICCS 2011

Demand-driven Movement Strategy for Moving Beacons in Distributed Sensor Localization

Anindya Iqbal * and Manzur Murshed

Gippsland School of Information Technology, Monash University, Churchill Vic 3842, Australia

Abstract

In a wireless sensor network, range-free localization with a moving beacon can reduce susceptibility to communication noises while concomitantly eliminate need for large number of expensive anchor nodes that are vulnerable to malicious attacks. This paper presents a moving beacon aided range-free localization technique, which is capable of estimating the location of a sensor with high accuracy. A novel distributed localization scheme is designed to optimally determine beacon movement strategy according to user demand. Superiority of this scheme to the state-of-the-art has been established in terms of location estimation quality, measured by the theoretical expected maximum error and simulated mean error while optimizing the beacon location density or traversal path length.

Keywords: sensor network; localization; range-free localization; moving beacon;

1. Introduction

Wireless Sensor Networks (WSNs) are usually deployed in a random fashion throughout a large unattended area to sense data of interest. Thousands of sensors, having limited sensing coverage and transmission capacity, sense specific properties from the surrounding environment to facilitate remote monitoring or detect the occurrence of expected events like fire. The sensed data are transmitted, periodically or on-demand basis, to the nearest base station for further processing. Unless the coverage of a WSN is confined to a small area, collecting sensed data without any information on locality makes little sense. For example, a bushfire detection network unable to pin-point the occurrence location will be of no help in a large geographical terrain such as the Australian outback. Locations of sensors are also indispensable requirement for many existing network traffic routing protocols. So, sensor locations need to be identified at an acceptable level of accuracy.

There are two straightforward ways to inform a sensor about its absolute geographic location, manually configuring it or equipping it with GPS, and neither is feasible. The former is not scalable and the latter is too expensive to implement. An acceptable solution has to rely on a distributed collaborative localization process where some of the nodes of the network are equipped with GPS to act as anchor nodes or beacons. These anchor nodes

* Corresponding author. Tel.: +61-3-5122-6138; fax: +61-3-5122-7137.
E-mail address: anindya.iqbal@monash.edu.

Selection and/or peer-review under responsibility of Prof. Mitsuhisa Sato and Prof. Satoshi Matsuoka
doi:10.1016/j.procs.2011.04.243

determine their locations with the help of GPS and transmit these to other nodes in the vicinity. The non-anchor nodes compute their locations based on these received beacon signals using a localization technique. There are alternative ways of centralised approaches where location computation is done at sink node. These approaches suffer from a single point of failure and traffic bottle-neck close to the sink. Hence distributed techniques are preferred by researchers in recent times.

Localization process varies depending on how the beacon signal is received and used thereafter [1]. Range-based techniques [2] try to estimate the absolute distance of sender and receiver by using one or more features of the transmitted signal e.g., received signal strength, time of arrival, angle, etc. While these techniques are likely to estimate sensor location accurately, they are quite vulnerable to environmental interference and signal fading, and the hardware required for determining absolute distance from received signal is also expensive. To avoid these shortcomings, range-free approaches avoid estimation of absolute distance and instead localize nodes from constraints like wireless connectivity and anchor proximity. The major limitation of range-free approaches is inaccuracy of location estimation as they only confine the possible location to the area of intersection of the fixed range of received beacon signals. To increase accuracy, number of anchor nodes need to be increased, which eventually increases the overall hardware cost. Accuracy of both the approaches is also affected by malicious anchor nodes broadcasting false location [2], [3]. These shortcomings are addressed by using moving beacon in [4]-[10].

In techniques using moving beacon, a single mobile beacon periodically broadcasts its position in the vicinity while traversing deployment area. If a non-anchor node receives beacon broadcast multiple times from different positions, it is more or less similar to receiving beacons from multiple anchors. The arrival and departure constraints of received beacons from upper and lower directions enable the sensor confine its potential location area [4]. The accuracy of location estimate depends on the distribution of beacon locations used by the moving beacon.

Galstyan *et al.* [6] first introduced an elementary localization technique using a moving beacon where location of a sensor is confined to the rectangular box bounded by a quadratic constraint from each received beacon signal. Xiao *et al.* [9], [4] proposed a more comprehensive localization scheme by restricting beacon mobility along horizontal and vertical lines only. However, the technique fails to attain the achievable accuracy as it considers the beacons from upper and lower directions separately to define two potential areas and use the average of their centres as the sensor location. Wu *et al*. [5] further refined this technique by introducing directional antennas with increased hardware cost. Teng *et al.* [8] recently introduced a probabilistic method to estimate location from randomly moving beacons and further refined the technique to reduce the number of beacon samples to achieve improved efficiency and accuracy. Kushwaha et al. [10] presented a scheme with acoustic signal based ranging technique using time-of-flight measurement. However, we have adopted radio signal strength based technique which is more widely used.

Moving beacons with auto-guided mobility such as a GPS-equipped transmitter on a robot is becoming a cost-effective solution for sensor localization covering a vast terrain that require frequent recalibration of locations as tiny sensor nodes may drift significantly over time due to wind, water flow, or other mobile entities such as grazing animals. Considering the sophistication of the mobile unit (e.g., an expensive robot), it is desirable that the process of localizing all sensor nodes is completed with the minimal beacon location density as well as minimal beacon traversal distance to reduce localization delay, conserve beacon's energy, and more importantly, save the expensive moving beacon from excessive wear and tear.

In schemes using moving beacon, traversal path length and transmission frequency depend on localization. The accuracy requirement is related to application scenario, e.g., military applications to monitor hidden explosives and environment monitoring schemes have quite different tolerance level of location estimation error. Whereas, high accuracy demands high beacon transmission density, low accuracy applications prefer conservation of energy used by movement and transmission of beacon. To deal with this trade off, a novel demand driven movement strategy is proposed in this paper where user can flexibly configure beacon's movement parameters and thereby minimize energy consumption or wear and tear.

When sensors are deployed with uniform random distribution, random mobility of the beacon node can be of little benefit as observed in [4], [5]. In order to guarantee that the process is not biased to any specific region or node, beacon locations must also be uniformly distributed and the moving beacon must move from one location to one of the neighbouring unvisited locations along the most-direct straight-line path.

In this paper, we have considered three tessellations [11] (triangular, rectangular, and hexagonal) of beacon locations to find an optimal beacon movement strategy to guarantee the expected maximum localization error within a user-defined bound. To the best of our knowledge, this optimization problem has not been studied before. In the

process of solving this problem, we have also developed a novel range-free distributed localization technique using rectangular tessellation of moving beacon locations, which outperforms the state-of-the-art in [4]. Specific contributions of this paper are as follows:

- Establishing that the rectangular tessellation of beacon locations is optimal among the three tessellations considered in terms of localizing randomly deployed sensors with uniform distribution.
- Developing a range-free sensor localization technique by constructing innermost intersection region from the received beacons and finding the centre of that region in such a way that the maximum distance of this centre from any sensor within that region is the minimum.
- Formulating a number of optimization problems on demand-driven beacon movement strategy and solving these NP-hard problems for finite-precision localization using the proposed localization scheme.
- Performing simulations to compare the proposed scheme against the state-of-the-art in [4] in realistic environment where signal distortion is modelled by combined path loss and shadow fading.

The proposed scheme can ideally achieve target expected maximum localization error using as much as 50% less beacon location density and 16% less beacon traversal path length, compared with [4] having the same computational complexity. Conversely, the proposed scheme can achieve target beacon location density with maximum 40% reduction in the expected maximum error. As analytical modeling of the mean localization error is impossible, we had to use extensive simulations to show that our proposed scheme enjoys on average 29% and 16% reduction in the mean localization error for ideal and realistic environment, respectively.

2. Optimal System Model

Sensors are deployed randomly in a field. The moving beacon traverses throughout the field and periodically transmits omni-directional beacons consisting of its instantaneous location. If a node receives a beacon signal, it is assumed to be within the radio transmission range R of that beacon.

In a performance study of deployment factors in wireless mesh networks, Robinson and Knightly [11] observed that the hexagonal tessellation requires double node density to achieve worst-case coverage probability identical to that by the triangular or rectangular tessellations. Although localization of any sensor requires coverage from at least two beacon locations, this observation is also valid in this context. Moreover, the optimal length of beacon traversal path is 9% to 54% longer for the hexagonal tessellation compared to that for rectangular one, which can be shown as follows:

With the rectangular tessellation of unit rectangle $\Delta x \times \Delta y$ m^2, $\Delta x \leq \Delta y$, a geographic area of $H \times V$ m^2 can be traversed optimally with path length of

$$L_{Rec} = H \times \frac{V}{\Delta y} = \frac{HV}{\Delta y}\ m. \qquad (1)$$

With the hexagonal tessellation of the same worst-case coverage, unit hexagon of side $b = \sqrt{(\Delta x)^2 + (\Delta y)^2}/2$ m must be used, as shown in Fig. 1. As two successive side traversal of $2b$ m constitutes only $3b/2$ m of horizontal displacement and the height of the unit hexagon is $\sqrt{3}b$ m, the optimal path length to traverse all the beacon locations in the same geographic area will be

$$L_{Hex} = \frac{H}{3b/2} \cdot 2b \times \frac{V}{\sqrt{3}b} = \frac{8\sqrt{3}}{9} \frac{HV}{\sqrt{(\Delta x)^2 + (\Delta y)^2}} m. \qquad (2)$$

Considering the two extremes, $\Delta x = \Delta y$ and $\Delta x \ll \Delta y$, we get

$$\frac{4\sqrt{6}}{9} \leq \frac{L_{Hex}}{L_{Rec}} \leq \frac{8\sqrt{3}}{9}. \qquad (3)$$

Although no significant difference can be drawn on the triangular and rectangular tessellations [11] in terms of optimal beacon node density and beacon traversal length, considering the simplicity of moving along horizontal and vertical directions only, the latter is preferred as evidenced in the existing techniques [4], [5].

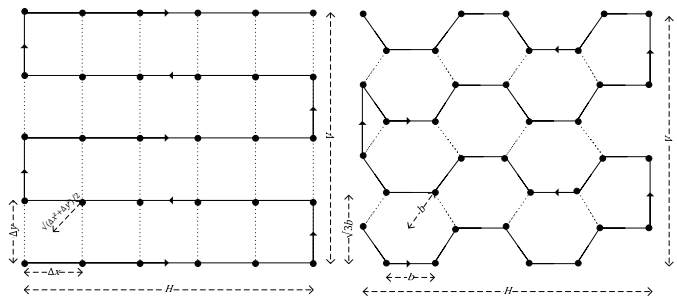

Fig. 1. Optimal traversal path of the moving beacon on rectangular and hexagonal tessellation of beacon loactions.

Another key observation in [11] is that moderate grid perturbation of (say) one-fifth inter-node distance has only 2% decrease in coverage area. We may then conclude that inaccuracies in positioning the moving beacon on exact locations due to terrain irregularity will have little impact on the expected maximum localization error.

3. Determining Location of a Sensor

3.1. Localization Using Arrival and Departure Information

When the beacon moves along a path and transmits beacon, the sensors that fall within the transmission range receives beacon signals. Depending on value of Δx and Δy, each sensor may receive multiple signals with respective beacon position from both upper and lower directions.

From the signals received, the first and last one from each direction is significant in localization process. These are termed differently in previous works from which we have adopted *arrival* and *departure* position (of beacon) for the first and last received signals, respectively. The sensors also receive current value of Δx and Δy from beacon transmission. So, it can also calculate the immediate position of the beacon before arrival and the immediate position after departure. These are termed as *pre-arrival* and *post-departure* position, respectively. The mechanism, by which a sensor may decide from which vertical direction a signal comes, is discussed in [4] and we refer readers to that work for limited space.

3.2. Our Algorithms

We have devised Algorithm 1 to determine the *Innermost Intersection Region* (IIR) of pre-arrival, arrival, departure, and post-departure beacon signals from both directions in a distributed way. Each sensor will use this scheme to find its possible location area.

Representative points on each circle as mentioned in line 3 of Algorithm 1 refer to the points that will define the intersection region. Its granularity is an implementation issue related to accuracy of area to determine or smoothness of the arcs. In our implementation, the points were taken at angular distance of 5° to compute areas. However, only the intersecting points of participating circles provide the minimal set of representative points that are used to find centres of these regions using a greedy heuristic presented in Algorithm 2.

Once an IIR is found, a sensor may reside at any point within this region. To specify the possible location, we propose the *polygon centre* as defined below.

Definition 1: *Centre point of a polygon is a point within that polygon such that maximum possible distance of this centre from all points within or on the polygon is the minimum.*

As the furthest point of any internal point of a polygon is one of its vertices, the following lemma holds.

Lemma 1: *Centre point of a polygon is a point within that polygon such that maximum possible distance of this centre from all vertices of the polygon is the minimum. That is, centre point of a polygon with n vertices* $V = \{v_1, v_2, \ldots v_n\}$ *is* $p = \operatorname{argmin}_{\forall q \text{ on or inside } P} \max_{1 \le i \le n} \|q - v_i\|$. ■

Algorithm 1 P_I = IIR(C)

Precondition: Set of eight equiradial circles of radius R, $C = \{c_{bpa}, c_{ba}, c_{bd}, c_{bpd}, c_{tpa}, c_{ta}, c_{td}, c_{tpd}\}$ where $c_{bpa}, c_{ba}, c_{bd}, c_{bpd}$ represent pre-arrival, arrival, departure, and post-departure circles, respectively, at the bottom row and $c_{tpa}, c_{ta}, c_{td}, c_{tpd}$ represent the same at the top row such that

$$\left.\begin{array}{c} centre(c_{bpa})_x + \Delta x = centre(c_{ba})_x \le centre(c_{bd})_x = centre(c_{bpd})_x - \Delta x \\ centre(c_{bpa})_y = centre(c_{ba})_y = centre(c_{bd})_y = centre(c_{bpd})_y \\ centre(c_{tpa})_x + \Delta x = centre(c_{ta})_x \le centre(c_{td})_x = centre(c_{tpd})_x - \Delta x \\ centre(c_{tpa})_y = centre(c_{ta})_y = centre(c_{td})_y = centre(c_{tpd})_y = centre(c_{bpa})_y + \Delta y \end{array}\right\}.$$

Postcondition: Polygon P_I representing the intersection area such that any of its interior point p is interior to circles $C_{ba}, C_{bd}, C_{ta}, C_{td}$, exterior to circles $C_{bpa}, C_{bpd}, C_{tpa}, C_{tpd}$, and $centre(c_{bpa})_y \ge p_y \ge centre(c_{tpa})_y$.

1. $P_I = \emptyset$;
2. **for** each circle $c \in C$ **do**
3. **for** each representative point p on c **do**
4. **if** $\|p - centre(c_{ba})\| \le R$ and $\|p - centre(c_{bd})\| \le R$ and $\|p - centre(c_{ta})\| \le R$ and $\|p - centrectd\le R$ and $p-centrecbpa\ge R$ and $p-centrecbpd\ge R$ and $p-centrectpa\ge R$ and $\|p - centre(c_{tpd})\| \ge R$ and $centre(c_{bpa})_y \le p_y \le centre(c_{tpa})_y$ **then**
5. $P_I = P_I \cup \{p\}$;
6. **end if**
7. **end for**
8. **end for**
9. Gravitational centre, $gc = \left(\sum_{\forall p \in P_I} \frac{p_x}{|P_I|}, \sum_{\forall p \in P_I} \frac{p_y}{|P_I|}\right)$;
10. Sort P_I with respect to the angle induced by gc.

Algorithm 2 p_c = POLYGON_CENTRE (V)

Precondition: A polygon with n vertices $V = \{v_1, v_2, \ldots v_n\}$.

Postcondition: Centre point p_c of the polygon such that the maximum distance of p_c from all vertices of the polygon is the minimum.

1. **for** each possible triangle $T_i \in V \times V \times V$ **do**
2. $p_c = \text{argmin}_{q \in \text{TRIANGLE\_CENTRE}(T_i)} \max_{1 \le i \le n} \|q - v_i\|$
3. **end for**

Algorithm 3 t_c = TRIANGLE_CENTRE (T)

Precondition: A triangle T.

Postcondition: Centre point t_c of T such that the maximum distance of t_c from all three vertices of T is the minimum.

1. **if** T is an obtuse triangle **then**
2. t_c= mid-point of the largest edge of T;
3. **else**
4. t_c= intersection point of perpendicular bisectors of the edges of T;
5. **end if**

The TRIANGLE_CENTRE( ) function used in Algorithm 2 is defined in Algorithm 3. Note that actual intersection region is a polygon of semi-circular arcs; whereas we have proposed estimating the centre of this area using a polygon of straight lines having the same vertices. We now establish that no error is induced due to this.

Let arc $\overline{AB}$ denote the complementary of arc AB such that $\overline{AB} + AB$ represents the entire corresponding circle. For example, if AB is the minor arc induced by chord AB to a circle, $\overline{AB}$ is the corresponding major arc and vice versa.

Lemma 2: *Three arcs AB, BC, and CA represent an IIR only if they are inscribed in circle ABC.*

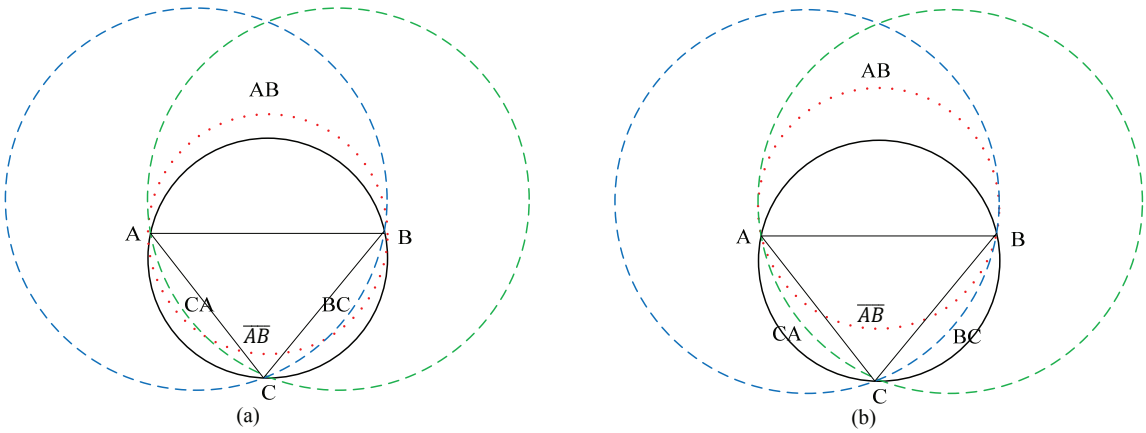

Fig. 2. Arc $\overline{AB}$ (a) intersects BC and CA inside inscribed circle; (b) creates new IIR with BC and CA.

Proof. Of the three arcs, let arc AB be not inscribed in circle ABC. For each circle having AB as a chord, either the minor or the major arc, induced by AB, will be exclusively inscribed in circle ABC. So, arc $\overline{AB}$ is now inscribed in circle ABC. If this arc $\overline{AB}$ intersects with any of the arcs BC and CA inside circle ABC (see Fig. 2(a)), the region marked by arcs AB, BC, *and* CA can no longer represent an IIR. Otherwise, as the region defined by arcs $\overline{AB}$, BC, *and* CA is fully enclosed in the region defined by *arcs* AB, BC, *and* CA, the former will be an IIR instead of the latter (see Fig. 2(b)). Hence, the lemma is proved by the transposition rule of inference. ■

Theorem 3: *Centre point of an IIR, comprising a polygon of arcs, minimizing the distance from all vertices coincides with the centre of a polygon of straight lines having the same set of vertices.*

Proof. Any IIR represented by three arcs AB, BC, *and* CA are confined to circle ABC by Lemma 2. As the centre of circle ABC is used as the centre of this IIR in Algorithm 3, no point in the boundary of this IIR can be further than the radius of circle ABC. So, the theorem is proved for polygons of three arcs. As the centre of a polygon having more than three arcs is calculated using all possible polygons of three arcs in Algorithm 2, the theorem holds for all polygons in general. ■

Computational complexity of our location estimation technique differs marginally from the same in [4]. In fact both the techniques are of constant order. Order of Algorithm POLYGON_CENTRE for a polygon with n vertices is $O(n^4)$. Order of Algorithm IIR is constant as only eight circles are considered to find the intersection area, which is represented by a polygon of at most eight vertices (empirically verified) and thus require only $O(8^4)$ operations to find its centre. The location estimator in [4] considers two polygons of at most five vertices; centre of each is then estimated in $O(5)$ operations. Note that the order of Algorithm IIR, common in both the approaches, is dominant in the whole process.

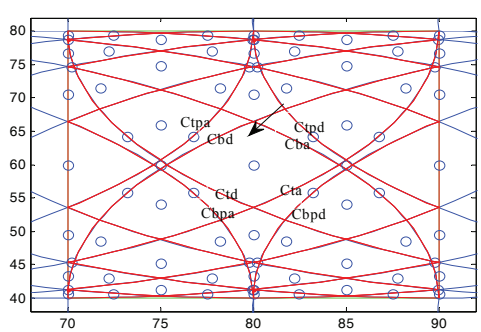

Fig. 3. Polygon center for different intersection regions drawn with our algorithms where $\Delta x = R/4$ and $\Delta y = R$.

Fig. 3 presents a programmatically drawn example of polygon centres for respective IIRs where the small circles represent sensors' location according to our proposed approach. One of the intersection regions is marked with arrow in Fig. 3 and pre-arrival, arrival, departure, and post-departure beacon signals represented by circles from both vertical directions are shown for this region. Although, the figure is drawn with ideal beacon transmission position and circular shapes, our approach successfully work in realistic scenario as it actually works with intersecting points of received beacons. This is supported by our simulation result presented in Section 5.

The way we have identified sensor location is quite different from the approach by Xiao *et al.* [4] where a possible location is determined for each individual half arrival-departure overlap (HADO) areas separately and then their midpoint is set as estimate position. In Fig. 4 this process is depicted with an example. The marker 'o' and '+' refer to positions obtained from lower and upper HADOs, respectively and '*' denotes the final sensor location determined as the midpoint of two HADO centres. The IIR of these HADOs is pointed with arrow in this figure and final sensor location must reside within this area. However, [4] failed to locate it within that area. Note that, they had to work only for R and $2R$ horizontal/vertical intervals with their centre computation scheme for specific shape of HADO, which is a naive approach. We investigated both the schemes for a wide range of horizontal/vertical intervals and thus formulated the novel demand-driven strategy.

For many intersection regions, our approach and that proposed in [4] produce same location, but in some cases they give inaccurate estimation as depicted in Fig. 4 As we have already discussed, in reality sensors identifying an intersection region reside at any point within it, it is not possible to theoretically estimate the average error of localization. However, we may compute the *expected maximum error* ($\overline{E_{\max}}$) of all regions for each set of values of Δx and Δy for both the approaches where

$$\overline{E_{\max}} = \sum_{\forall \text{ Intersection region } I} \frac{Area(I)}{\sum_{\forall \text{Intersection region } J} Area(J)} \times \max_{\text{vertex } v \text{ of } I} \|POLYGON\_CENTRE(I) - v\| \qquad (4)$$

For the approach proposed by Xiao *et al.* [4], to compute $\overline{E_{\max}}_{xiao}$ their corresponding estimated sensor location is considered in place of $POLYGON\_CENTRE\ (I)$.

4. Demand-driven Beacon Movement Strategies

Quality of localization can be estimated as the mean localization error or the expected maximum localization error or the average area of intersection, to name a few. It is, however, impossible to model the mean localization error in any analytical framework. As the rectangular tessellation of beacon locations is shown optimal in Section 2 in terms of both beacon location density and beacon traversal path length to achieve a target worst-case coverage, we are interested in the following two optimization problems on the rectangular tessellation:

minimize beacon location density, $\frac{HV}{\Delta x \Delta y}$ given expected maximum localization error, $\overline{E_{\max}} \leq T_{\text{error}}$. (5)

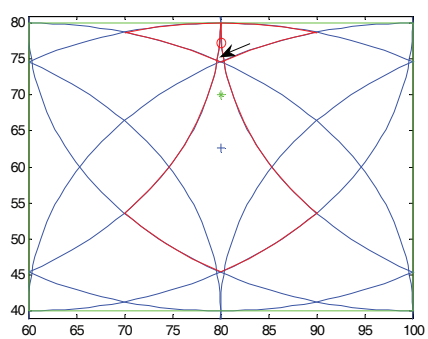

Fig. 4. An example scenario of sensor location found by [4].

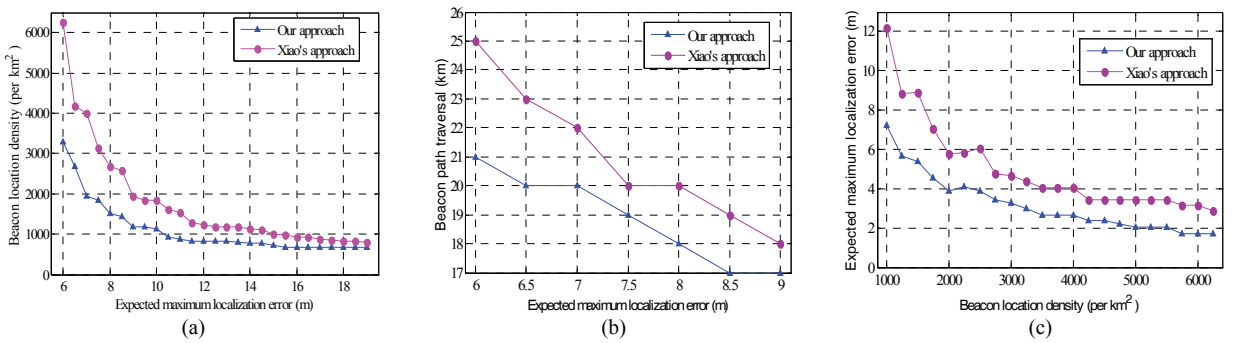

Fig. 5. Comparison between proposed and Xiao's [4] schemes on (a) Beacon location for different expected maximum error target; (b) Beacon traversal path length for different expected maximum error target; (c) Expected maximum localization error for different beacon density.

$$\textbf{minimize}\ \text{beacon traversal path length}, \frac{HV}{\Delta y}\ \text{given expected maximum localization error}, \overline{E_{\max}} \leq T_{\text{error}}. \qquad (6)$$

where T_{error} is a user-defined error threshold. There are many similar optimization problems that have been considered but not reported in this paper due to lack of space. For example, instead of seeking the expected maximum localization error within a threshold, the user might be interested in guaranteeing the average area of intersection within a threshold.

As all these problems are NP-hard, instead of finding any closed-form solution, we have to look at their restricted versions where Δx and Δy are constrained with finite precision. With finite precision, it is possible to consider a finite number of possible values for Δx and Δy to populate a table of quality of localization estimators such as the expected maximum localization error and the average area of intersection. Solving any of the abovementioned optimality problems is then translated to simply inspecting this off-line table to find the optimal setup satisfying the given constraint.

Fig. 5(a) and (b) present comparative performance of our proposed and Xiao's [4] schemes in terms of beacon location density and beacon traversal path length, respectively, against demand-driven $\overline{E_{\max}}$ values. In both cases, the proposed scheme shows considerable superiority achieving target error using as much as 50% less beacon location density and 16% less beacon traversal path length.

For the sake of completeness, we have also included solution to the dual of the optimization problem in (5), formulated as

$$\textbf{minimize}\ \text{expected maximum localization error}, \overline{E_{\max}}\ \text{given beacon location density}, \frac{HV}{\Delta x \Delta y} \leq T_{\text{density}}. \qquad (7)$$

Fig. 5(c) presents comparative performance on the above optimization problem. Again, the proposed scheme shows considerable superiority achieving target beacon location density with expected maximum localization error as much as 40% less.

5. Simulation

Although our proposed location estimator is designed to minimize the maximum error, its performance evaluation in terms of minimizing mean error of randomly placed nodes is highly significant as that represents the practical scenario. Our approach is likely to perform well in this consideration as well against Xiao's approach [4] which estimates sensor locations, in many cases, outside the intersection areas; whereas our approach always confines locations within the intersections areas; in the extreme on their boundaries. To validate this by comparing the performance of our proposed localization technique with that of Xiao's we simulated WSNs in MATLAB. Performance is also compared in realistic environment where path loss and shadow fading increases localization error. All the results presented here are computed from average of 100 simulation runs.

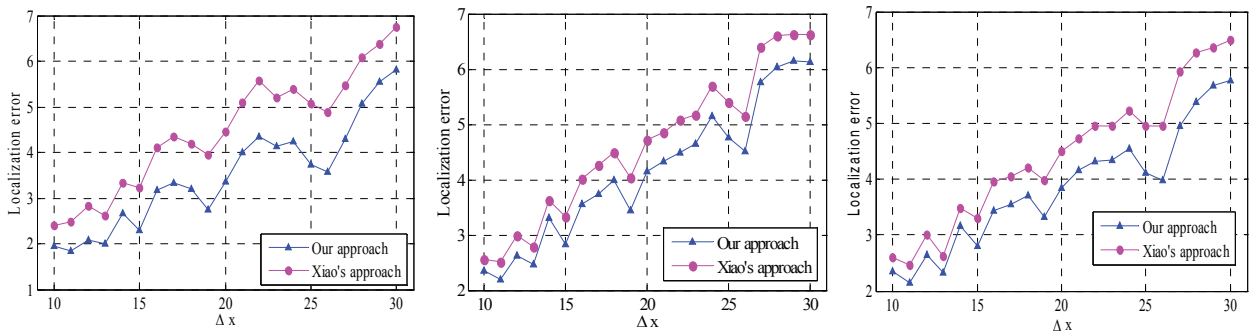

Fig. 6. Localization error for different Δx values when (a) no fading effect, (b) $\gamma = 2$ and $\sigma = 4$, and (c) $\gamma = 3$ and $\sigma = 2.5$.

5.1. Simulation Setup

We have considered wireless sensors deployed in a representative area where all possible types of intersection regions from transmitted beacon signals are available. To accommodate all shapes the total representative area varied with Δx. To keep sensor density uniform despite variable areas, we placed number of nodes 10 times the area in square meters each time. The maximum transmission range of this beacon is $R = 40$. These nodes receive beacon signals and compute own location from those.

To model realistic environment where sensors may miss some of the arrival or departure beacon signals due to wireless signal attenuation, we used combined path loss and shadow fading. Transmission beacon of radius R may be affected according to (8) where the path loss component γ is assumed to be 2, which is standard for free space propagation. The standard deviation $\sigma$of normally distributed random shadow fading for free space propagation is considered 4 dB [2] when high fading is present. We have also experimented in high path loss and low fading environment considering $\gamma = 3$ and $\sigma = 2.5$ dB. The mean distance affected by fading is used from [2] as:

$$\bar{\epsilon} = \left(1 - 10^{-\frac{\sigma}{10\gamma}}\right) R. \qquad (8)$$

Each arc of intersecting polygons have $\bar{\epsilon}$ width of areas potentially affected by fading spreading equally in both sides of the arc. Hence, within a region the probable affected area's width may be approximated as $\bar{\epsilon}/2$ along all arcs. Since shadow fading affects a transmission signal in Gaussian distributed way with mean 0, a sensor node within this area again has equal probability of being actually affected or not. We have used uniform random probability to determine if a sensor within this area is affected, i.e. misses either arrival or departure signal and then the sensor will consider itself to reside in the adjacent region. Consequently, centre of the adjacent region will be estimated as its location and consequently localization error is likely to increase.

5.2. Results and Discussion

Localization techniques are evaluated by their induced error both in ideal environment and realistic one. In the abovementioned simulation setup we tested our approach and that of Xiao [4] varying path loss or shadow fading parameters.

Fig. 6(a) presents mean localization error in ideal environment with no fading effect. The beacon transmission intervals varied as $\Delta x = R/4$ to $3R/4$ when $\Delta y = R$. These Δx values are reasonable since shorter values cause very frequent transmissions incurring high cost. Moreover, created IIRs for these values are of such areas that small part of the area has the risk of missing the arrival/departure beacons. That's why in our experiment, we considered only one signal may be missed by a sensor at any instance. Localization error increased for both the approaches with increase in Δx and this is explainable by the consequent increase in size of IIRs. We perform better in all instances with mean gain more than 29%.

Fig. 6(b) shows performance of both approaches in high fading scenario. Although we outperform Xiao's approach in all cases, the margin of mean gain is reduced to 12.5%. The reason is comprehensible from the observation that the regions (refer to Fig. 4) have a pattern where every region asymmetric with respect to x-axis is surrounded by symmetric regions and Xiao's centres are mostly affected for these asymmetric regions. As we showed that some of Xiao's centres go outside the corresponding intersection region, it goes close to centre of the one of its adjacent regions. Recall here that due to fading, a sensor takes the location of adjacent centre. Hence, for the sensors near the common arc with this adjacent region, Xiao's centre is close to the fading-affected centre. Consequently, in such cases Xiao's approach has less error increase compared to that of ours. Fig. 6(c) shows similar performance when path loss is high and fading is low. Here our mean gain is almost 16%.

6. Conclusion

In this paper we have presented a moving beacon-aided range-free localization scheme which follows a novel demand-driven optimal movement strategy to conserve localization time and cost of unnecessary path traversal and beacon transmissions. The beauty of our technique is the flexibility with which the beacon may dynamically decide movement parameters on user demand. Our scheme achieves as much as 40% improvement in terms of the expected maximum localization error and on average 29% reduction in the mean error with uniformly distributed random sensor deployment compared to the state-of-the-art [4] without increase in computational complexity. In realistic environment also, modelled with fading and path loss, the superiority is retained at reduced level. In future we may compare our scheme with other approaches such as where beacon itself computes location and then transmit it.

References

1. G. Mao, B. Fidan, and B. Anderson, "Wireless sensor network localization techniques," Computer Networks, 51(10)(2007), 2529–53.
2. A. Iqbal and M. Murshed, "Attack-Resistant Sensor Localization under Realistic Wireless Signal Fading," In Proc. of IEEE Wireless Communication and Networking Conf. (WCNC), 2010.
3. A Srinivasan and J Wu, "A survey on secure localization in wireless sensor Networks," Computer Networks, 52(12)(2008).
4. B. Xiao, H. Chen, and S. Zhou, "Distributed localization Using a Moving Beacon in Wireless Sensor Networks," IEEE Transactions on Parallel and Distributed Systems, 19(5)(2008).
5. Y-H. Wu and W-M Chen, "Localization of Wireless Sensor Networks Using a Moving beacon with Directional Antenna," In Proc. of IEEE Intl. Conf. on High performance Computing and Communications (HPCC), 2009.
6. A. Galstyan, B. Krishnamachari, K. Lerman, and S. Pattem, "Distributed Online Localization in Sensor Networks Using a Moving Target," In Proc. of Intl. Symposium of Information Processing in Sensor Networks (IPSN), 2004.
7. N. Priyantha, H. Balakrishnan, E. Demaine, and S. Teller, "Mobile-Assisted Localization in Wireless Sensor Networks," In Proc. of IEEE Intl. Conf. on Computer Communications (Infocom), 2005.
8. G. Teng, K. Zheng, and W. Dong, "Adapting Mobile Beacon-Assisted Localization in Wireless Sensor Networks," Journal of Sensors, 9(2009), 2760–79.
9. B. Xiao, H. Chen, and S. Zhou, "A Walking beacon Assisted Localization in Wireless Sensor Networks," In Proc. of IEEE Intl. Conf. on Communications (ICC), 2007.
10. M. Kushwaha, K. Molnar, J. Sallai, P. Volgyesi, M. Maroti, and A. Ledeczi, "Sensor Node Localization Using mobile Acoustic Beacons," In Proc. of IEEE Conf. On Mobile Ad-hoc and Sensor Systems (MASS), 2005.
11. J. Robinson and E. Knightly, "A Performance Study of Deployment Factors in Wireless Mesh Networks," In Proc. of IEEE Intl. Conf. on Computer Communications (Infocom), 2007.